

Chemi-ionization in collisions of metastable neon with argon*

R. H. Neynaber and G. D. Magnuson

Intelcom Rad Tech, P. O. Box 80817, San Diego, California 92138

(Received 21 October 1974)

Absolute and relative cross sections were obtained for the Penning-ionization (PI) reaction $\text{Ne}^* + \text{Ar} \rightarrow \text{Ne} + \text{Ar}^+ + e$ and the associative-ionization (AI) reaction $\text{Ne}^* + \text{Ar} \rightarrow \text{NeAr}^+ + e$ by a merging-beams technique over a range of interaction energies W from 0.01 to 600 eV. The Ne^* represents a composite of $\text{Ne}(3s^3P_2)$ and $\text{Ne}(3s^3P_0)$. The PI cross section Q_{Ar^+} rises with decreasing W except for a small dip near 0.05 eV and exhibits a rather weak dependence on W . For a change of almost five orders of magnitude in W , Q_{Ar^+} only changes by about a factor of 7. The AI cross section Q_{NeAr^+} monotonically increases with decreasing W and shows a large dependence on W . The Q_{NeAr^+} at $W = 0.01$ eV is about 70 times larger than that at 0.5 eV. The total cross section $Q_T = Q_{\text{Ar}^+} + Q_{\text{NeAr}^+}$ is compared with theoretical and other experimental values. At low W our absolute Q_T are considerably larger than those of Tang, Marcus, and Muschlitz although the relative Q_T for both experiments are in fair agreement.

I. INTRODUCTION

In order to learn more about the role of the relative kinetic energy of motion of reactants W in chemi-ionization reactions from near thermal to higher energies, we have used merging beams to measure relative and absolute cross sections for the Penning-ionization (PI) reaction



and the associative-ionization (AI) reaction



The Ne^* represents $\text{Ne}(3s^3P_2)$ and $\text{Ne}(3s^3P_0)$. These states have energies of 16.62 and 16.71 eV, respectively, and were not separated in the experiment. The PI reaction is exothermic by 0.86 eV for $\text{Ne}(3s^3P_2)$ and by 0.96 eV for $\text{Ne}(3s^3P_0)$.

Studies of reaction (1a) were made in the range $0.01 \leq W \leq 600$ eV by measuring the product Ar^+ current and lab-energy distributions of Ar^+ . Cross sections for reaction (1b) were obtained over the range $0.01 \leq W \leq 0.5$ eV from measurements of the NeAr^+ current.

Laboratory energies of the species in these reactions will be designated by E with an appropriate subscript. For example, the lab energy of Ne^* will be E_{Ne^*} .

II. EXPERIMENTAL

The merging-beams apparatus was like that described previously,¹ except a demerging magnet was used instead of a condenser, a retarding grid was inserted in the detector assembly between the electrostatic hemispherical analyzer and the electron multiplier, and both reactant beams were chopped. The Ne^* beam was modulated at 330 Hz

by electrically chopping the Ne^+ beam from which it was generated. The Ar beam was mechanically chopped at 230 Hz. The lock-in amplifier was tuned to the difference frequency of 100 Hz. The retarding grid was used to study reaction (1a). Its potential was adjusted to prevent undesired Ar^+ (principally from the reactant Ar stripping in residual gas) from reaching the multiplier and also to transmit Ar^+ arising from the reaction. The grid was not necessary for reaction (1b), and its potential was simply adjusted for 100% transmission of the product NeAr^+ .

Electron bombardment sources 1 and 2 (see Ref. 1) were used for generating Ne^+ and Ar^+ , respectively. The energy of the ionizing electrons in the Ne^+ source was about 40 eV and in the Ar^+ source about 25 eV. The Ar^+ was converted to Ar in the first charge-transfer cell (see Ref. 1), which contained Ar or H_2 . The Ne^* was converted to Ne in the second charge-transfer cell which contained Na vapor.

Generally the energy of the Ne^+ was fixed and the energy of the Ar^+ was adjusted to give the desired W . A potential could be applied to the interaction region so that product ions formed inside the region would, upon leaving it, have a different energy than those formed outside. The detector assembly could then be adjusted to accept only ions formed inside the interaction region.

III. BEAM COMPOSITION

The use of Ar (or H_2) in the first charge-transfer cell allowed a resonant (or near-resonant) charge-transfer reaction to occur in which ground-state Ar^+ from source 2 was converted to ground-state Ar. Since this reaction predominated in the cell, it is assumed that the Ar beam consisted of

ground-state particles.

Sodium vapor was used in the second charge-transfer cell because it resulted in small energy defects for the near-resonant charge transfer conversion of ground-state Ne^+ to the $3s\ ^3P_2$ and $3s\ ^3P_0$ metastable states of Ne. The energy defects for these states are -0.20 and -0.29 eV, respectively. The energy defects for charge-transfer conversion of Ne^+ to the $3s\ ^3P_1$, $3s\ ^1P_1$ and $3p\ ^3S_1$ states of Ne are -0.25 , -0.42 , and -1.96 eV, respectively. The energy levels of these states are the closest three to the metastable levels.

From theoretical, asymmetric charge-transfer curves obtained by Rapp and Francis,² it appears reasonable to assume that differences in the cross sections for the formation of the $3s\ ^3P_2$, $3s\ ^3P_1$, $3s\ ^3P_0$, and $3s\ ^1P_1$ states due to differences in energy defects are negligible. If it is further assumed, in the absence of more detailed knowledge, that the cross sections are proportional to the statistical weights of the above four states, then these cross sections are in the ratios 5:3:1:3. Cross sections for the formation of the $3p\ ^3S_1$ state and all other states would be negligible.

The $3s\ ^3P_1$ and $3s\ ^1P_1$ states can make allowed transitions to the $2p\ ^6S_0$ ground state of Ne, and in our experiments virtually all of these states decayed in this way before reaching the interaction region. Therefore, at the interaction region only $\text{Ne}(3s\ ^3P_2)$, $\text{Ne}(3s\ ^3P_0)$, and $\text{Ne}(2p\ ^6S_0)$ existed and were in the ratios 5:1:6. Consequently, under the assumption of a statistical distribution, the ratio of metastable to ground-state species in the Ne beam was unity. The value of this ratio is a factor in determining absolute cross sections for reactions (1a) and (1b), and any error in the ratio will result in an equal error in these cross sections. However, relative cross sections depend only on the ratio remaining fixed.

For our studies with He^+ beams^{1,3,4} we invoked the work of Donnally and Thoeming⁵ and Schlachter *et al.*⁶ to support the assumption of a statistical distribution of singlet and triplet states. We are not aware of similar studies for neon.

IV. METHOD

The desired W can be achieved by making the magnitude of the lab velocity of Ar, $|\vec{v}_{\text{Ar}}|$, appropriately greater or less than that of Ne^* , $|\vec{v}_{\text{Ne}^*}|$. Kinematics for reaction (1a) and for the case $|\vec{v}_{\text{Ar}}| < |\vec{v}_{\text{Ne}^*}|$ are shown by the Newton diagram of Fig. 1.

Since only energy distributions of the product Ar^+ were measured for reaction (1a), information was obtained on $|\vec{v}_{\text{Ar}^+}|$ but not on the directional properties of \vec{v}_{Ar^+} . Therefore, α and θ (see Fig. 1)

were not specifically determined. A comparison of the values $|\vec{v}_{\text{Ar}^+}|$ with $|\vec{v}_c|$ can be used, however, to assign rough limits to θ .

In the center-of-mass system, θ is defined as the angle between the velocity of Ar, \vec{V}_{Ar} , and the velocity of Ar^+ , \vec{V}_{Ar^+} . Scattering in the center-of-mass system along the original Ar direction (i.e., $\theta = 0^\circ$) will be defined as forward scattering, whereas scattering opposite to the original Ar direction (i.e., $\theta = 180^\circ$) will be defined as backscattering.

The lab energy of NeAr^+ in reaction (1b) is monoenergetic since this particle is formed by the coalescence of two heavy particles with the emission of an electron whose momentum is negligible. The lab velocity of NeAr^+ is equal to the velocity of the center of mass.

The general method of obtaining relative and absolute cross sections has been described previously¹ and includes determining areas under lab-energy distributions. In addition to this method, another technique was used in which lab-energy distributions did not have to be measured. With this technique all of the product ions were collected in one measurement. This was achieved by reducing the resolution of the electrostatic hemispherical energy analyzer in the detector assembly. A similar method was used in some of our earlier merging-beams experiments.^{7,8} When used for the same cross-section determination, both methods agreed within experimental error. For both of these techniques the potential of the retarding grid was reduced so that saturation was achieved for the product ions transmitted by the hemispherical analyzer.

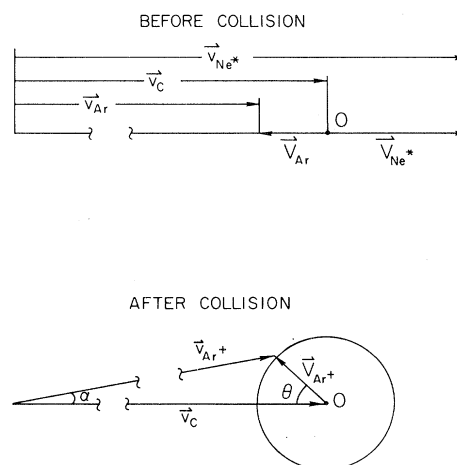


FIG. 1. Newton diagrams for $\text{Ne}^* + \text{Ar} \rightarrow \text{Ne} + \text{Ar}^+ + e$. Subscript c refers to the c.m., \vec{v} is for laboratory velocity, and \vec{V} is for velocity in the c.m. system. The scattering angle in the lab system is α ; in the c.m. system it is θ . The drawing is not to scale.

As mentioned previously, relative cross sections require that the ratio of metastable to ground-state species in the Ne beam remain constant. To ensure this constancy we kept E_{Ne^*} fixed and adjusted E_{Ar} to obtain a desired W for relative cross-section measurements. We also fixed the Na-cell pressure for such measurements.

The usual tests were made to ensure the validity of the cross-section measurements.⁹ These included tests which (i) showed no loss of product ions by angular scattering, (ii) indicated 100% transmission of the detector assembly for product ions over the entire lab-energy range that was covered in the experiments, (iii) showed linearity of the product-ion currents with primary beam currents, and (iv) established the independence of cross sections upon E_{Ne^*} and E_{Ar} for the same W .

Measurements were more difficult for reaction (1a) than (1b), and these harder measurements were subject to more errors. For this reason additional tests were made for (1a). These included verification that, with E_{Ne^*} fixed, cross sections were independent of the gas and the gas pressure in the cell associated with charge transfer of Ar^+ to Ar. In addition to H_2 and Ar, Kr was used in the cell. For example, it was shown that the ratio of the cross section at $W=1$ eV to that at $W=100$ eV (i.e., Q_1/Q_{100}) was the same for each of these gases. As another example, the pressure of Ar in the cell was varied from 0.27 to 1.9 μm with no change observed in Q_1/Q_{100} . Finally, it was shown that the cross section at $W=1$ eV was independent of H_2 pressure in the cell over the range 0.6–2 μm . Typical operating pressures for Ar or H_2 in the cell were 1–2 μm .

Other tests that were made for reaction (1a) included the observation of the independence of cross sections on the pressure of Na in the second charge-transfer cell. For example, the ratio of the cross section at $W=100$ eV (i.e., Q_{10}/Q_{100}) was constant within experimental error for pressures in the range 0.2–2 μm . In addition, the cross section at $W=100$ eV was independent of Na pressure in the range 0.7–2 μm . Typical operating pressures of Na vapor were 1–2 μm .

Again with respect to reaction (1a), if stripped Ar from the reactant beam would have passed through the retarding grid and reached the detector, an incoherent current would have been generated. If by some means the stripped Ar had been cross modulated by the Ne beam, a coherent current would have resulted and been confused with the desired Ar^+ from the reaction. To determine whether this unlikely series of events occurred, the Ne^* beam was turned off and arrangements were made so that the Ar beam would simultaneously be chopped at 230 and 330 Hz. With the

lock-in amplifier tuned to the difference frequency of 100 Hz, coherent stripped Ar currents were observed at the detector. The dependence of these currents on such parameters as potential of the retarding grid, pressure in the detection chamber (normally 1×10^{-7} Torr), current through the coils of the demerging magnet, and energy setting of the detector were determined. These dependences were compared with those of Ar^+ currents from reaction (1a). The results were so different that the possibility of cross-modulated stripped Ar significantly affecting measurements of Ar^+ for reaction (1a) can be eliminated.

We temporarily improved the collimation of the merged beams to observe the effect on measurements. The improvement was made by increasing the separation of the first and second collimating apertures (see Ref. 1). No discernible difference was detected in either absolute or relative cross-section determinations.

As a final check on the operation of the apparatus, relative and absolute cross sections were measured for the charge-transfer reaction $\text{Ar}^+ + \text{Ar} \rightarrow \text{Ar} + \text{Ar}^+$ over the range $0.1 \leq W \leq 10$ eV. The study of this reaction required the use of the retarding grid, and the problems associated with the measurements were similar to those for reaction (1a). The measured cross sections were in reasonable agreement (10–20%) with those obtained with our apparatus in a similar study in 1967,⁷ which in turn were in fair agreement with the theoretical results of Rapp and Francis.²

V. RESULTS AND DISCUSSION

A. Energy distributions

Laboratory-energy distributions of Ar^+ production from $\text{Ne}^* + \text{Ar}$ are shown in Fig. 2. Distributions were not measured below $W=0.1$ eV because of poor signal-to-noise ratios.

The full width at half-maximum of a distribution in Fig. 2 at a given W and E_{Ar} is about the same as would be obtained from the measured distribution of a monoenergetic Ar^+ beam at an energy equal to E_{Ar} . In addition, a distribution in the figure, except for the rather low-intensity, high-energy tail, has about the same shape as that arising from a monoenergetic Ar^+ beam. Finally, the energy at the peak of a distribution in the figure is approximately equal to E_{Ar} . The peak energy can be determined within an error of about ± 5 eV.

These facts indicate that the reaction is directed with most of the Ar^+ scattering in the center-of-mass system approximately in the direction of Ar (i.e., $\theta \approx 0^\circ$). Furthermore, there is little momentum transfer in the c.m. so that the energy of the reactant Ar is about the same as that of the prod-

uct Ar^+ and $W' \approx W$, where W' is the total relative kinetic energy of the heavy products. [When $W' = W$, the exothermicity of reaction (1a) will be taken up by the kinetic energy of the released electron.]

Because the scattering circle for Ar^+ after the collision (see Fig. 1) is very small at low W , small errors in measuring the peak energy of a distribution can cause difficulty in estimating W' and θ . These problems would be most severe for the distribution at $W = 0.1$ eV, where a difference in the peak E_{Ar^+} of a few electron volts can make a difference in W' of 15% or so and a difference in θ of perhaps 20° . For $W \geq 1$ eV errors of several electron volts in E_{Ar^+} have negligible effect on W' and θ .

The high-energy tails of the distributions in Fig. 2 could represent angular scattering of Ar^+ in the center-of-mass system. Rough limits on θ can be determined by comparing the E_{Ar^+} of a point in a distribution with $E_{\text{Ar}^+}^c$, which is defined as the energy of Ar^+ if it had the velocity of the c.m. For example, for $W = 10, 100$, and 300 eV, the E_{Ar^+} is always less than $E_{\text{Ar}^+}^c$, and therefore $\theta < 90^\circ$ (see Fig. 1). For $W = 0.1$ and 1 eV, E_{Ar^+} in the tails can be greater or less than $E_{\text{Ar}^+}^c$, and so θ can be less than or greater than 90° . This behavior is not unreasonable since more intimate collisions might be expected for lower W , and larger θ 's can occur for closer collisions.

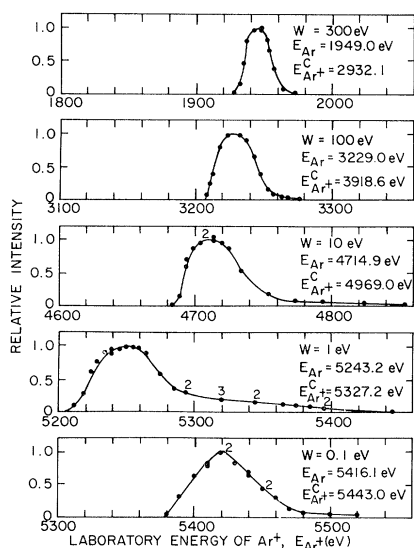


FIG. 2. Laboratory-energy distributions of Ar^+ production from $\text{Ne}^* + \text{Ar}$. For all distributions Ne^* is faster than Ar , and $E_{\text{Ne}^*} = 2750$ eV. The energy of Ar^+ if it had the velocity of the c.m. is designated as $E_{\text{Ar}^+}^c$. A digit adjacent to an experimental point represents the number of times that value was obtained.

The lab-energy distributions of NeAr^+ in reaction (1b) are not shown. As mentioned previously, NeAr^+ is monoenergetic.

B. Relative cross sections

Relative cross sections Q_{Ar^+} for Ar^+ production from collisions of Ne^* and Ar are shown in Fig. 3. The measurements were obtained by a method described previously in which all of the Ar^+ for a given W was collected in one measurement. Another technique also mentioned above was to measure the lab-energy distribution of the Ar^+ and, from the area under the distribution, obtain a cross section. This latter method gave Q_{Ar^+} similar to those in Fig. 3.

The possibility that some of the Ar^+ is due to collisional ionization of Ar by ground-state Ne or Ne^* must be considered. Since E_{Ar^+} for collisional ionization is different from E_{Ar^+} for PI, we were able to look for evidence of collisional ionization by varying the resolution of the detector. We did this for $W \leq 400$ eV and saw none. We made no such tests for $W > 400$ eV because of greater difficulty in achieving the required resolution.

We are not aware of any measurements for such reactions. However, if it is assumed that the cross sections for these processes are similar to those for the ionization of N_2 and O_2 by N_2 and O_2 as measured by Utterback,^{10,11} then it is conceivable that collisional ionization cannot be neglected compared to PI for $W > 400$ eV. In summary, for $W \leq 400$ eV, the Q_{Ar^+} in Fig. 3 are for PI. For $W > 400$ eV, the Q_{Ar^+} shown may not be solely due to PI.

For Fig. 3, Ne^* was faster than Ar . The cross sections were obtained with different conditions for $W \leq 100$ eV and $W \geq 100$ eV. For both energy regimes the Q_{Ar^+} were normalized to the cross section at $W = 100$ eV, which for Fig. 3 was arbitrarily

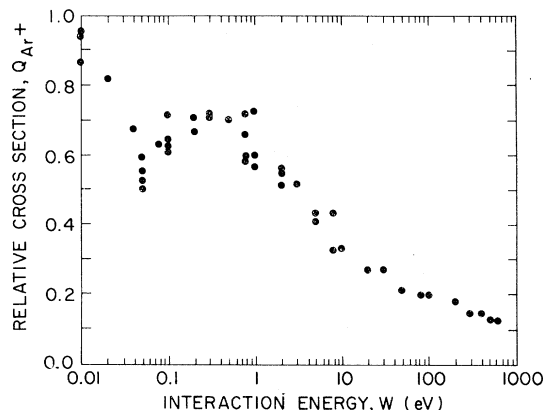


FIG. 3. Relative cross sections for Ar^+ production from $\text{Ne}^* + \text{Ar}$.

chosen as 0.2. For $W \leq 100$ eV, E_{Ne^*} was fixed at 2750 eV and for $W \geq 100$ eV, E_{Ne^*} was fixed at 4200 eV. If E_{Ne^*} had been 2750 eV for $W > 100$ eV, the E_{Ar} would have been too small to generate sufficiently large Ar^+ beams from the Ar^+ source.

At $W = 100$ eV the ratio of the cross section with $E_{\text{Ne}^*} = 2750$ to that with $E_{\text{Ne}^*} = 4200$ was determined to be unity within experimental error. This suggests that the fraction of Ne^* in the neutral neon beam is essentially the same for these two conditions.

As mentioned previously, it was advisable to make relative cross-section measurements with E_{Ne^*} fixed, as was done for the Q_{Ar^+} of Fig. 3. However, we made some Q_{Ar^+} measurements over the W range of Fig. 3 with E_{Ar} fixed at 5000 eV. The relative curve had a shape very similar to that of Fig. 3.

We estimate that transverse velocities¹² increase our nominal, or quoted, W 's in these experiments by an energy W_T no greater than 0.005 eV. A $W_T = 0.005$ eV could result in percentage reductions of Q_{Ar^+} of 18, 7, and 2 for nominal W 's of 0.01, 0.03, and 0.1 eV, respectively.

Random errors for Q_{Ar^+} are larger for the smaller W , where signal-to-noise ratios were smaller. It is estimated these random errors are about $\pm 15\%$ for $W \leq 1$ eV and $\pm 10\%$ for $W > 1$ eV.

As mentioned previously, the lab-energy distributions of Ar^+ reflect little momentum transfer in the c.m. This is also the case for resonant charge-transfer reactions. From Fig. 3 we note another qualitative similarity with resonant charge transfer. This is the rather weak dependence of the cross section on W . For a change of almost five orders of magnitude in W , Q_{Ar^+} only changes by about a factor of 7. Later (from Figs. 4 and 5) a third likeness will be noted, viz., that the PI cross sections are relatively large, e.g., about $3.4 \times 10^{-15} \text{ cm}^2$ for $W = 0.01$ eV. At present, the significance of these observations, if any, is unknown.

Relative cross sections Q_{NeAr^+} for reaction (1b) are shown as squares in Fig. 4. Some of these cross sections were obtained from areas under energy distributions; others were determined by the technique described previously in which distributions did not have to be measured.

The AI cross sections in Fig. 4 were made with E_{Ne^*} fixed at 2000 eV. An energy of Ne^* of $E_{\text{Ne}^*} = 2750$ eV, as was used to determine Q_{Ar^+} at the lower W in Fig. 3, could not be employed because voltages on the detector assembly (see Ref. 1) required for NeAr^+ detection would have been above the design limits of the assembly. Random errors for Q_{NeAr^+} are estimated at $\pm 10\%$.

To relate the magnitudes of the AI and PI cross

sections to each other, the ratio $r = Q_{\text{NeAr}^+}/Q_{\text{Ar}^+}$ was measured at $W = 0.1$ eV and will be designated $r(0.1)$. For the AI measurement, $E_{\text{Ne}^*} = 2000$ eV and for the PI measurement, $E_{\text{Ne}^*} = 2750$ eV. It was assumed that the fraction of Ne^* in the neutral neon beams was the same for $E_{\text{Ne}^*} = 2000$ eV and $E_{\text{Ne}^*} = 2750$ eV. This was not proved explicitly, but a good indication of the validity of the assumption resulted from a cross-section ratio we had measured earlier in this study. This was the ratio of $Q_{\text{Ar}^+}(10)$ [where $Q_{\text{Ar}^+}(10)$ is the PI cross section at $W = 10$ eV] with $E_{\text{Ne}^*} = 2129$ eV and $E_{\text{Ar}} = 5000$ eV (Ne^* slower than Ar) to $Q_{\text{Ar}^+}(10)$ with $E_{\text{Ne}^*} = 2904$ eV and $E_{\text{Ar}} = 5000$ eV (Ne^* faster than Ar). Within experimental error this ratio was unity, as it should be for a constant fraction of Ne^* .

The value of $r(0.1)$ was determined to be 0.19 ± 0.03 . The cross section for PI relative to that for AI can be determined at any W from $r(0.1)$, Fig. 3, and the AI cross section in Fig. 4. The PI cross sections relative to the AI are shown in Fig. 4. In addition, the sum of the AI and PI cross sections is shown. This sum will be designated as the total ionization cross section Q_T . Above $W = 0.2$ eV, Q_T is essentially the same as Q_{Ar^+} . Random errors in Q_T are about ± 15 or 16% for $W \leq 1$ eV.

C. Absolute cross sections

Two absolute cross sections were obtained. One of these was $Q_{\text{Ar}^+}(10) = 1.6 \times 10^{-15} \text{ cm}^2$ and the other was $Q_{\text{NeAr}^+}(0.1) = 3.5 \times 10^{-16} \text{ cm}^2$.

As before, $E_{\text{Ne}^*} = 2000$ eV for the AI measurement and $E_{\text{Ne}^*} = 2750$ eV for the PI measurement. For the reasons presented previously, it was again assumed that the fraction of Ne^* in the neutral neon beam was the same for both conditions. This fraction was taken as $\frac{1}{2}$, the value resulting from the previously discussed assumption of a statistical distribution of singlet and triplet states of neon in the beams.

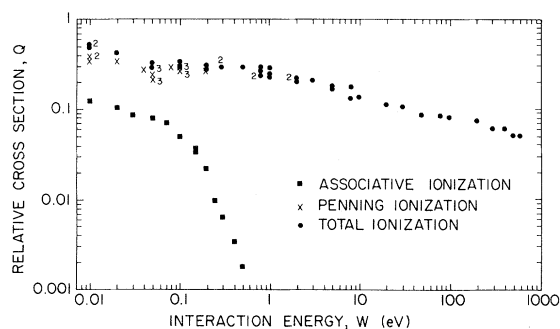


FIG. 4. Cross sections Q_{Ar^+} , Q_{NeAr^+} , and Q_T relative to each other for $\text{Ne}^* + \text{Ar}$ collisions. A digit adjacent to a point represents the number of times that value was obtained.

Another factor that was used in the determination of the two absolute cross sections above was the secondary electron emission coefficient for Ne^* , γ_{Ne^*} . This was assumed to be 16% larger than the coefficient for Ne^+ , γ_{Ne^+} , at the same energy. Measurements of γ_{Ne^+} were made in our experiment, but we are not aware of any measurements of γ_{Ne^*} . The basic assumption is that the coefficients for neon behave like those for helium, and it is known from measurements by Layton¹³ that $\gamma_{\text{He}^*}/\gamma_{\text{He}^+} = 1.16$.

To determine if the two absolute cross sections above are consistent with each other within experimental error, another value of $Q_{\text{NeAr}^+}(0.1)$ was determined from the value of $Q_{\text{Ar}^+}(10)$, the Q_{Ar^+} curve of Fig. 3, and $r(0.1)$. This new $Q_{\text{NeAr}^+}(0.1) = 5.8 \times 10^{-16} \text{ cm}^2$. Although this is somewhat different from the first value, the errors associated with each $Q_{\text{NeAr}^+}(0.1)$ would overlap. This demonstrates the rather large experimental errors associated with our absolute measurements.

An average of the two $Q_{\text{NeAr}^+}(0.1)$ values is taken as our best determination with the result that $\overline{Q}_{\text{NeAr}^+}(0.1) = 4.7 \times 10^{-16} \text{ cm}^2$ with estimated errors of +41% and -32%. This error is a composite of systematic and random errors. The systematic error consists of +25% in the overlap integral. The random error is assumed to be $\pm 32\%$. Systematic errors associated with the fraction of metastables in the neutral neon beam and with γ_{Ne^*} are not included in the estimated error.

Absolute values for $Q_{\text{NeAr}^+}(W)$, $Q_{\text{Ar}^+}(W)$, and $Q_T(W)$ can be obtained from the above value for $\overline{Q}_{\text{NeAr}^+}(0.1)$ and the data shown in Fig. 4. Absolute $Q_T(W)$ are shown in Fig. 5. The estimated errors for these $Q_T(W)$ are +41% and -32% which do not include estimates of the errors for the fraction of metastables or γ_{Ne^*} . In addition to our data, we have shown the beam-gas results of Tang *et al.*¹⁴ (TMM) and of Moseley *et al.*¹⁵ (MPLH) and the theoretical curve of Olson.¹⁶ In Olson's calculation the coupling-width parameter was adjusted so that the cross-section curve would best fit the data of TMM.

It is noted in Fig. 5 that in the energy regions of overlap, our relative Q_T are in fair agreement with those of the two beam-gas experiments. This agreement is particularly interesting at low W where it can be seen that the shallow depression observed by TMM is not inconsistent with our results.

Our absolute Q_T at high W are about 35 to 50% lower than those of MPLH. The errors associated with the beam-gas results are from ± 15 to $\pm 20\%$. The error brackets associated with the Q_T of each experiment overlap at $W = 80 \text{ eV}$ and almost overlap at all other W 's without considering possible

errors for the fraction of metastables or γ_{Ne^*} .

On the other hand, at low W our absolute Q_T are from 6 to 8 times larger than those of TMM. As indicated by TMM in their note added in proof, a more accurate value of γ (for thermal Ne^* on a gas-covered gold surface) than theirs was obtained by Dunning and Smith.¹⁷ This value of γ is approximately twice as large as that of TMM, and, if applicable to the results of the latter, would raise the Q_T of TMM by a factor of about 2. We have recently been advised by Muschlitz¹⁸ that his group has made some preliminary remeasurements of γ for the TMM surface with the result that the new γ is about three times larger than the original TMM value. This now leads Muschlitz to believe that the Q_T of TMM could be too low by about a factor of 3. It appears that obtaining a fairly accurate value of γ for a thermal beam, as in the TMM experiment, is more difficult than for a fast beam as in our work.

If the Q_T of TMM were raised by a factor of three, the discrepancy between our results and those of TMM would be reduced to a factor of from 2 to 2.7. However, the error brackets for the two experiments would still not overlap. The TMM-quoted error in Q_T (exclusive of the error in γ) is $\pm 5\%$. Any adjustment of the fraction of metastables or of γ_{Ne^*} in our experiment to make our results agree better with those of TMM would produce larger differences between our results and those of MPLH (see Fig. 5). Our relative Q_T make it impossible to agree (within the mutual errors of the experiments) in absolute value with both the results of TMM and those of MPLH.

Measurements leading to Q_T near 300 K have been made by others, and the results are compiled in a discussion by Lampe¹⁹ of ionization in collisions of excited reactants. All of these measurements were made more than two decades ago. The

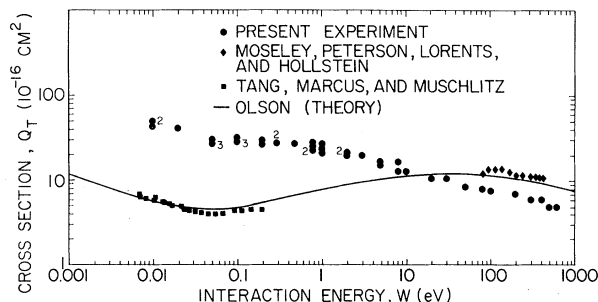


FIG. 5. Cross sections for production of both Ar^+ and NeAr^+ from $\text{Ne}^* + \text{Ar}$. A digit adjacent to an experimental point represents the number of times that value was obtained. Included are the results of the present experiment, the beam-gas data of Tang *et al.* (Ref. 14) and of Moseley *et al.* (Ref. 15), and the theoretical curve of Olson (Ref. 16).

values cover a range from about $8 \times 10^{-18} \text{ cm}^2$ (Hoffmann²⁰; conductivity measurements of a Ne-Ar mixture excited by a discharge) to $3.0 \times 10^{-15} \text{ cm}^2$ (Kruithof and Penning²¹; determination of Townsend ionization coefficient at breakdown potential for a Ne-Ar mixture). The most recent of these early measurements were those of Biondi²² and of Phelps and Molnar.²³ Biondi obtained a $Q_T = 2.6 \times 10^{-16} \text{ cm}^2$ by using microwave techniques to study ionization in Ne-Ar mixtures following a pulsed discharge. Phelps and Molnar determined that $Q_T = 2 \times 10^{-16} \text{ cm}^2$ from optical absorption techniques. From these diverse results support can be found for either the TMM or the present experimental Q_T . It is very difficult to choose the most accurate Q_T from these values.

It is interesting to note that when γ is not involved in the measurements of the Muschlitz group the results appear to agree with ours. We have already shown how the shape of the Q_T versus W curve for the TMM and the present experiment supports this. Other supporting evidence of this is observed in a comparison of the branching ratio $R = Q_{\text{NeAr}^+}/Q_T$ from our work and that from other experiments of the Muschlitz group by Kramer

*et al.*²⁴ The R for the experiment of Kramer *et al.* was determined at 330 K, which corresponds to $W = 0.033 \text{ eV}$ for our experiment. They obtained $R(330 \text{ K}) = 0.36 \pm 1.5\%$. Our value can be obtained from Fig. 4 and is $R(0.033) = 0.28 \pm 28\%$. These two values of R agree within the mutual errors of the experiments. These observations suggest the possibility that the discrepancy between our results and those of TMM is associated with γ and that perhaps the real γ for the TMM work is even more than three times larger than the old γ .

For the theoretical Q_T , Olson used a Morse potential and, as mentioned previously, adjusted the coupling width in the calculation so that his theoretical curve would fit the TMM data. We have found that our low-energy data can be fit with a different choice of Olson's coupling width. However, our high-energy results would then be smaller than the theoretical values much as they are in Fig. 5. From Olson's work⁶ it appears that a Lennard-Jones (L-J) potential at higher energies would more closely fit our data. Olson believes, however, that an L-J potential at the higher energies has a core that is too repulsive.

*Research sponsored by the Office of Naval Research under Contract No. N00014-74-C-0011, NR012-115 and by the Air Force Office of Scientific Research (AFSC), U.S. Air Force under Contract No. F44620-74-C-0002.

¹R. H. Neynaber, G. D. Magnuson, and J. K. Layton, *J. Chem. Phys.* **57**, 5128 (1972).

²D. Rapp and W. E. Francis, *J. Chem. Phys.* **37**, 2631 (1962).

³G. D. Magnuson and R. H. Neynaber, *J. Chem. Phys.* **60**, 3385 (1974).

⁴R. H. Neynaber and G. D. Magnuson, *J. Chem. Phys.* **61**, 749 (1974).

⁵B. L. Donnally and G. Thoeming, *Phys. Rev.* **159**, 87 (1967).

⁶A. S. Schlachter, D. H. Loyd, P. J. Bjorkholm, L. W. Anderson, and W. Haeberli, *Phys. Rev.* **174**, 201 (1968).

⁷R. H. Neynaber, S. M. Trujillo, and E. W. Rothe, *Phys. Rev.* **157**, 101 (1967).

⁸R. H. Neynaber and S. M. Trujillo, *Phys. Rev.* **167**, 163 (1968).

⁹R. H. Neynaber, G. D. Magnuson, S. M. Trujillo, and B. F. Myers, *Phys. Rev. A* **5**, 285 (1972).

¹⁰N. G. Utterback and G. H. Miller, *Phys. Rev.* **124**, 1477

(1961).

¹¹N. G. Utterback, *Phys. Rev.* **129**, 219 (1963).

¹²S. M. Trujillo, R. H. Neynaber, and E. W. Rothe, *Rev. Sci. Instrum.* **37**, 1655 (1966).

¹³J. K. Layton, *J. Chem. Phys.* **59**, 5744 (1973).

¹⁴S. Y. Tang, A. B. Marcus, and E. E. Muschlitz, Jr., *J. Chem. Phys.* **56**, 566 (1972).

¹⁵J. T. Moseley, J. R. Peterson, D. C. Lorents, and M. Hollstein, *Phys. Rev. A* **6**, 1025 (1972).

¹⁶R. E. Olson, *Chem. Phys. Lett.* **13**, 307 (1972).

¹⁷F. B. Dunning and A. C. H. Smith, *J. Phys. B* **4**, 1696 (1971).

¹⁸E. E. Muschlitz, Jr., University of Florida (private communication).

¹⁹F. W. Lampe, *Ion-Molecule Reactions*, edited by J. L. Franklin (Plenum, New York, 1972), Vol. 2, Chap. 13, pp. 601-646.

²⁰A. Hoffmann, *Z. Phys.* **119**, 223 (1942).

²¹A. A. Kruithof and F. M. Penning, *Physica (Utr.)* **4**, 430 (1937).

²²M. A. Biondi, *Phys. Rev.* **88**, 660 (1952).

²³A. V. Phelps and J. P. Molnar, *Phys. Rev.* **89**, 1202 (1953).

²⁴H. L. Kramer, J. A. Herce, and E. E. Muschlitz, Jr., *J. Chem. Phys.* **56**, 4166 (1972).